

Zone folding, morphogenesis of charge densities, and the role of periodicity in GaAs-Al_xGa_{1-x}As (001) superlattices

M. A. Gell, D. Ninno, and M. Jaros

Department of Theoretical Physics, The University of Newcastle upon Tyne, Newcastle upon Tyne NE1 7RU, England, United Kingdom

D. C. Herbert

Royal Signals and Radar Establishment, Saint Andrews Road, Great Malvern, Worcestershire WR14 3PS, England, United Kingdom

(Received 23 December 1985)

We have used our pseudopotential method to show the strong mixing and zone-folding effects which occur in superlattices comprised of ultrathin layers when zone-center- and zone-edge-related states cross. We present a detailed comparison with the experimental results of Ishibashi *et al.* and indicate how the energetics of this crossing can be linked to the relative alignment between the GaAs and AlAs band structures. Specifically, we suggest that X_0^c of AlAs lies about 0.3 eV below X_0^c of GaAs. In addition, we show that the superlattice periodicity governs the spectral character of the superlattice states and impresses optical anisotropy on the superlattice, even for those superlattices whose period is comprised of only two monolayers. We also illustrate a morphogenesis of charge density which is controlled by the way in which the superlattice period is divided up into the constituent layers. The polarized charge densities which may exist in superlattices comprised of very thin and ultrathin layers and which correspond to states which lie outside the commonly accepted picture of confinement may also be found in thick-layered systems. These polarized charge densities, together with optical anisotropy, provide a clear distinction between alloy mixtures and superlattices whose periods are comprised of only a few monolayers.

I. INTRODUCTION

Ishibashi *et al.*¹ have recently shown that, using metalorganic chemical vapor deposition, it is possible to grow GaAs-AlAs (001) superlattices of high quality comprised of very thin (≤ 100 Å) and ultrathin (≤ 20 Å) layers. The results which they present provide evidence for and information about the crossing of the ground zone-center- and zone-edge-related superlattice states. Significantly, the energetics of this crossing can be linked to the relative alignment of the GaAs and AlAs band structures. The experimental data of Ishibashi *et al.* are also very useful in that they are derived from superlattices ranging from those in which the width of the layers is a monolayer, defined here as one layer of anions plus one layer of cations, to those in which the superperiodicity is much longer than the underlying natural periodicity of the lattice. Some insight into the electronic properties of superlattices comprised of ultrathin layers has been provided by the pioneering theoretical work of Caruthers and Lin-Chung,² Pickett *et al.*,³ Schulman and McGill,⁴ Andreoni and Car,⁵ and Mon.⁶ However, a systematic comparison between experiment and theory has not been attempted since, until very recently, few experimental data have been available.

In this paper, we present a selection of our results on GaAs-AlGaAs superlattices comprised of mostly very thin and ultrathin layers which highlight certain important aspects of the work reported by Ishibashi *et al.* In particular, we show the effect of zone folding in GaAs-

AlAs (001) superlattices comprised of ultrathin layers. We demonstrate the role of superlattice periodicity and indicate how its effects compete with the effects of the relative widths of the different layers which make up the superlattice. We also illustrate a morphogenesis of charge density which is controlled by the way in which the superlattice period is divided up into the constituent layers. We show that the polarized charge densities which may exist in superlattices comprised of very thin and ultrathin layers and which lie outside the commonly accepted picture of confinement may also be found in thick-layered systems.

II. METHOD OF CALCULATION

In our method,^{7,8} a perturbation V is added to the Hamiltonian H_0 of a perfect infinite crystal such as GaAs. The perturbation V describes the changes in spin-orbit coupling and in local atomic potentials when pseudoatoms in the host crystal are substituted by different species in order to form the superlattice. The eigenfunctions ϕ_{nks} and eigenvalues E_{nks} of H_0 , such that $H_0\phi_{nks} = E_{nks}\phi_{nks}$, are generated by diagonalizing the matrix

$$\begin{aligned} & \left\| \left[\frac{1}{2}K^2 - E_{nks} \right] \delta_{\mathbf{G},\mathbf{G}'} \delta_{s,s'} \right. \\ & \left. + V_L(|\mathbf{G}-\mathbf{G}'|) \delta_{s,s'} + V_{s.o.}^{s,s'}(\mathbf{K},\mathbf{K}') \right\| = 0, \end{aligned}$$

where n is the band index, \mathbf{G} is a bulk reciprocal-lattice vector, wave vector $\mathbf{K} = \mathbf{k} + \mathbf{G}$, s and s' are spin states,

and V_L and $V_{s.o.}$ are the local and spin-orbit coupling terms. The effects of spin-orbit coupling have been incorporated using an extension of the method introduced by Weisz.^{9,10}

The superlattice wavefunction ψ is constructed as a linear combination of host Bloch functions; $\psi = \sum_{n,k,s} A_{nks} \phi_{nks}$. The Bloch functions which make up ψ are determined unambiguously since V is a periodic function. For a wave vector \mathbf{k}_{SBZ} in the superlattice Brillouin zone (SBZ), the only ϕ_{nks} which are included in the expansion of ψ are those which correspond to \mathbf{k} points in the bulk Brillouin zone (BBZ) which are coupled to \mathbf{k}_{SBZ} by some linear combination of superlattice reciprocal lattice vectors. Manipulation of the Schrödinger equation leads to the following eigenvalue equation which is solved by direct diagonalization

$$A_{n'k's'}(E_{n'k's'} - E) + \sum_{n,k,s} A_{nks} \langle \phi_{n'k's'} | V | \phi_{nks} \rangle = 0.$$

It should be noted that we are solving an integral equation and so avoid the necessity to impose boundary conditions for the matching of wave functions.

We have fitted form factors for GaAs and AlAs so that the relative positions of principal symmetry points in the band structures are in as good agreement with experiment as possible (see Table I). For GaAs, we have used the recent experimental data of Woford and Bradley¹¹ and for AlAs we have based the direct and indirect gaps on data available in Refs. 12–14. For simplicity, although this need not be a constraint, we have used the same lattice constant $A=10.683$ a.u. for both GaAs and AlAs. We use a value of $\Delta_0=0.334$ eV for the spin-orbit splitting at point Γ of GaAs and a value of $\Delta_0=0.296$ eV for AlAs. Where necessary, the virtual-crystal approximation has

TABLE I. Symmetric and antisymmetric form factors used to generate the band structures of GaAs and AlAs. The form factors are in a.u. The energies in eV at the bottom of the table correspond to the principal symmetry points in the lowest conduction band. To achieve 60:40 offsets, the band structure of AlAs is shifted so that the energy of its X_6^c point is 1.69 eV, i.e., 0.321 eV below the X_6^c point of GaAs.

q^2	AlAs	GaAs
	Symmetric	
3	-0.11537	-0.11980
8	0.01271	0.00630
11	0.03500	0.03000
12	0.00000	0.00000
	Antisymmetric	
3	0.03625	0.03500
4	0.03125	0.02500
11	-0.00375	0.00500
12	0.00000	0.00000
Points	AlAs	GaAs
Γ_6^c	3.020	1.523
X_6^c	2.290	2.012
L_6^c	2.661	1.846

been used to give the band structure of the alloy $\text{Al}_x\text{Ga}_{1-x}\text{As}$.

In order to control the relative alignment of the GaAs and AlAs band structures, the symmetric part $S(q)$ of the local potential $V_L(q)$ is adjusted at $q=0$. In the present calculations, we have adjusted $S(0)$ so that 60% of the difference between the band gaps (in Table I) of GaAs and AlAs at point Γ is taken up as the conduction-band offset, since it would appear from recent literature^{15–20} that the so-called 60:40 offset, or an offset which is close to it, is one which is generally favored for the GaAs-AlAs system. However, it should be noted that due to the variation in quoted values for the direct gap of AlAs, it is also necessary to state the value which has been assumed in order to define an unambiguous offset for the GaAs-AlAs system.

III. NUMERICAL RESULTS AND DISCUSSION

The period of the first superlattices which we consider here is equivalent to six lattice constants along the [001] direction and corresponds to about 34 Å. We have performed calculations in which the number M of GaAs layers range from 0 (AlAs) to 12 (GaAs). The number N of AlAs layers is given by $N=12-M$. Three perspectives of the unit cell of the $(\text{GaAs})_M(\text{AlAs})_{11}$ superlattice are given in Fig. 1. The experimental results of Ishibashi *et al.*¹ correspond to $(\text{GaAs})_M(\text{AlAs})_N$ superlattices for which $M=N$ and so, for this period, the only experimental data with which we make a direct comparison are those for the case $M=N=6$.

In Fig. 2, we show the energies of (a) the conduction and (b) the valence states closest to the band edges in the $[(\text{GaAs})_M(\text{AlAs})_N; M+N=12]$ superlattices. The energies associated with the principal symmetry points of GaAs and AlAs are indicated at the edges ($N=0$ and 12) of the figure. It should be noted that the superlattice wave function is based on a multiband, full-zone expansion and so at $N=0$ and $N=12$ in Fig. 2, energies corresponding to various bands at several \mathbf{k} points in the BBZ are shown. Since the period of the superlattice is equivalent to six lattice constants along the [001] direction, the \mathbf{k} points in the BBZ which are coupled to the center of the SBZ are those which lie on the Δ line and which have the form $\mathbf{k}=(2\pi/A), (0,0,0.166m)$ where m is a positive or negative integer. In Fig. 3, we show the charge densities associated with (a) the superlattice conduction states and (b) the superlattice valence states with $M=N=6$. The conduction states C_i are labeled with i increasing from the edge of the conduction band and the ordering of the charge densities corresponds to the ordering of the energy levels in Fig. 2 at $M=N=6$. An analogous system of labeling has been used for the valence states V_i . The charge densities are plotted along a line in the [001] direction which passes through mid-bond positions (see Fig. 1). In Table II, we show the leading coefficients, or, more precisely, the sum over electron spin of the moduli squared of the A_{nks} coefficients, in the expansion of the wave function of some of the states shown in Fig. 3. Since the sum over spin of the moduli squared of the A_{nks} coefficients is symmetric with respect to inver-

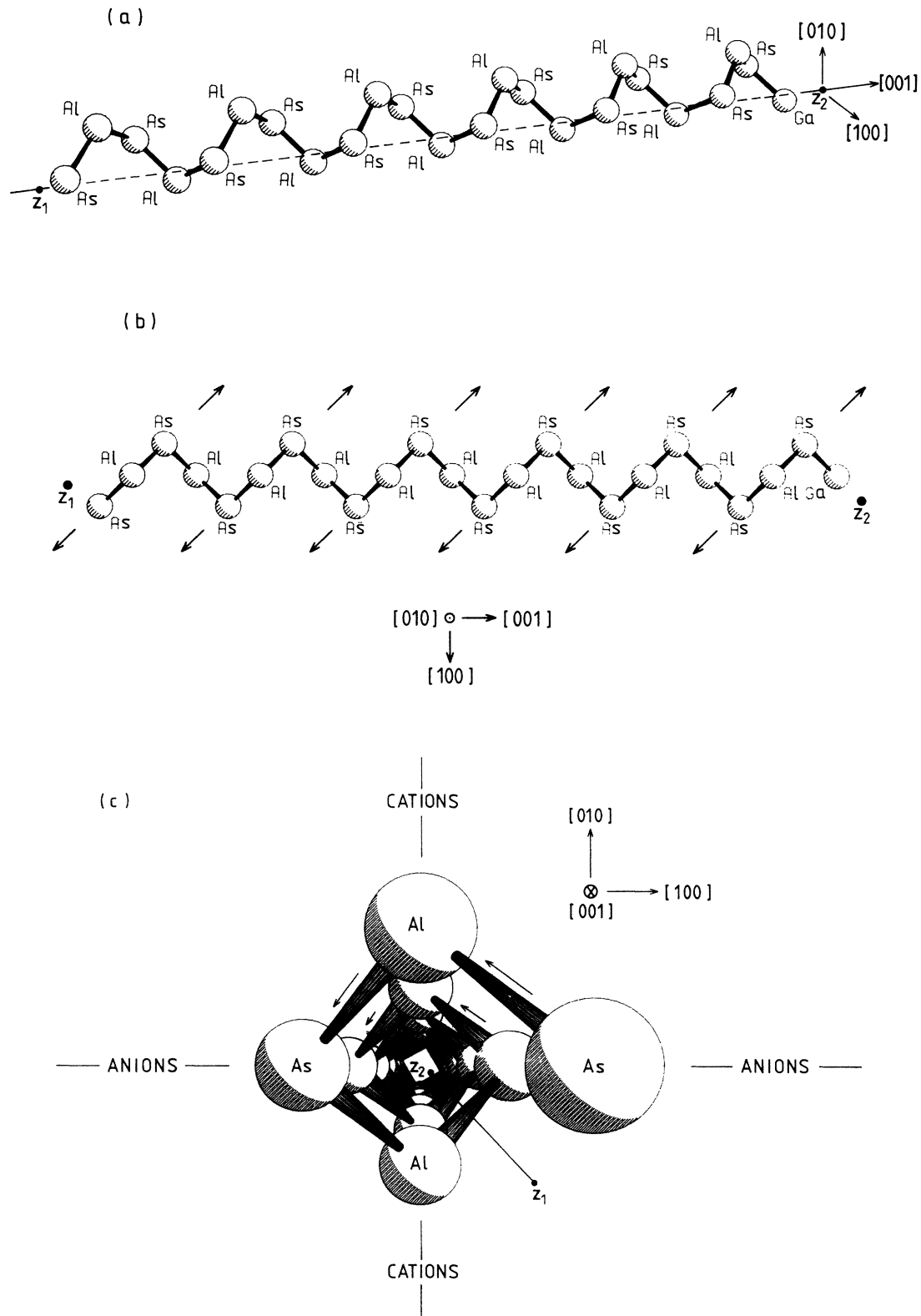


FIG. 1. Three perspectives of the atoms in the unit cell of the $(\text{GaAs})_1(\text{AlAs})_{11}$ superlattice. (a) A view in the $[-0.6, 0.3, 0.2]$ direction showing the line Z_1Z_2 passing through mid-bond positions along which the charge densities in Fig. 4 have been plotted. (b) A view in the $[0, -1, 0]$ direction. The charge densities in Fig. 5 have been plotted along the spiral of bonds between the points Z_1 and Z_2 . The arrows indicate the bonds along which the charge in state V2 of Fig. 5 is channeled. (c) A view in the $[001]$ direction. The planes of anions and planes of cations are indicated and the line Z_1Z_2 passing through mid-bond positions is shown. The arrows indicate the bonds along which the charge in state V2 of Fig. 5 is channeled.

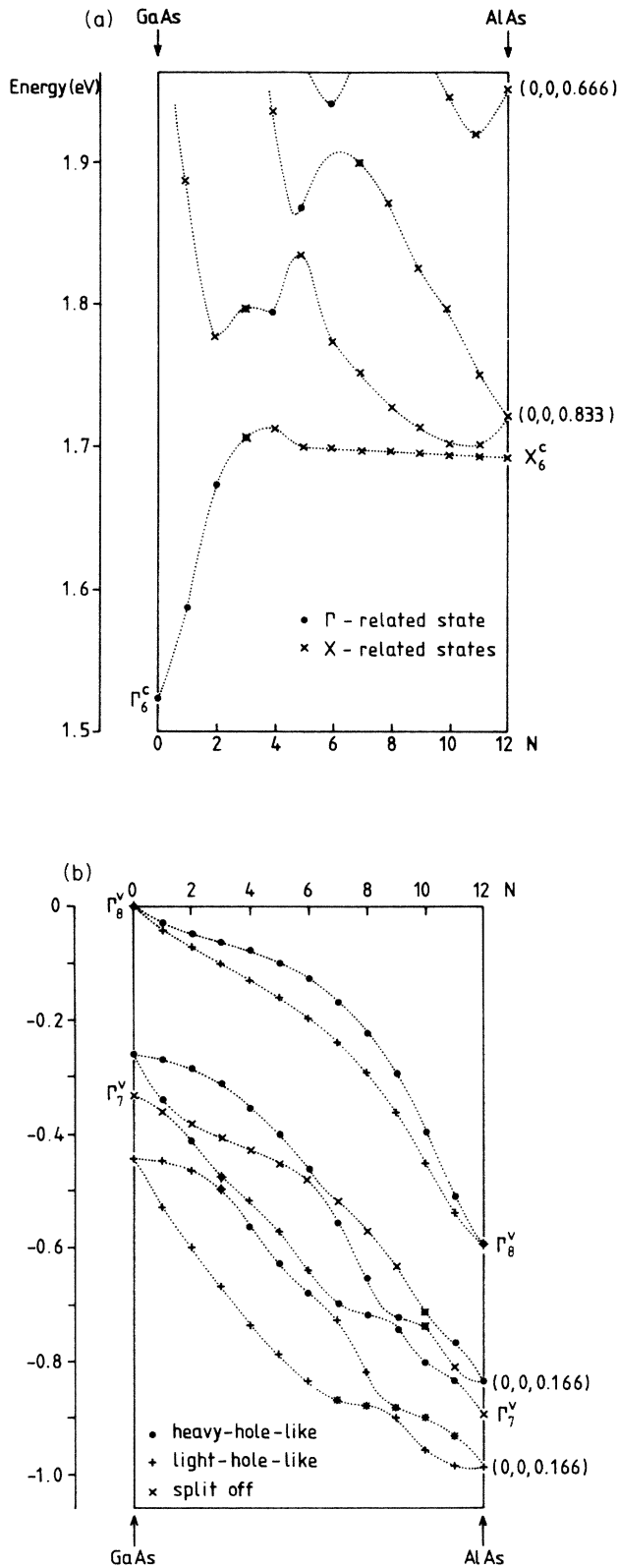


FIG. 2. Energies of (a) the conduction states and (b) the valence states closest to the band edges in the $[(\text{GaAs})_M(\text{AlAs})_N; M+N=12]$ (001) superlattices. The energies associated with principal symmetry points of GaAs ($N=0$) and AlAs ($N=12$) are shown at the edges of the figure. The dotted lines are merely a guide for the eye.

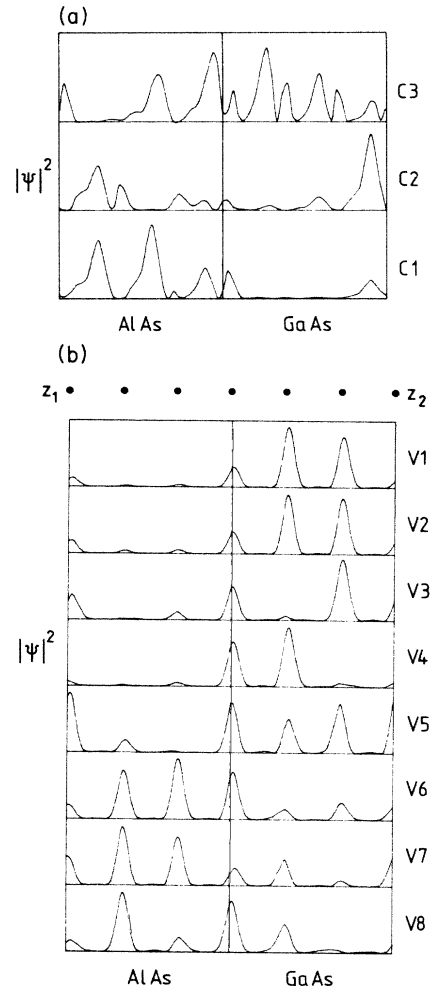


FIG. 3. Charge densities of (a) the conduction states and (b) the valence states at the center of the superlattice Brillouin zone for the $(\text{GaAs})_6(\text{AlAs})_6$ superlattice. The charge densities are plotted along the line Z_1Z_2 in the [001] direction [see Fig. 1(a)]. The mid-bond positions through which the line Z_1Z_2 passes are indicated in the figure (b). The peak of $|\psi|^2$ is set to 1 to facilitate presentation. The energies of the states are shown in Fig. 2 at $N=6$.

sion of \mathbf{k} , only those coefficients corresponding to \mathbf{k} points lying in the irreducible segment of the BBZ have been shown. For each superlattice state, the coefficients, normalized so that the largest coefficient is 1, are shown separately for the top three pairs of spin-degenerate bulk valence bands (VB2, VB3 and VB4) and for the bottom two pairs of spin-degenerate bulk conduction bands (CB1 and CB2). The labeling is such that VB2 corresponds to the bulk split-off bands, VB3 corresponds to the bulk light-hole bands, VB4 corresponds to the bulk heavy-hole bands and CB1 corresponds to the lowest conduction bands.

It can be seen from Figs. 2 and 3 and Table II that mixing between components from the center and edges of the BBZ in the $M=N=6$ superlattice is very strong. This is not surprising for a superlattice in which the layers are only about 17 Å wide and the separation between the closest zone-center (of GaAs) and zone-edge (of AlAs) minima is only about 180 meV. It is also clear from Fig.

TABLE II. Sum over spin of the moduli squared of the leading coefficients in the expansion of some of the states, shown in Fig. 3, in the $(\text{GaAs})_6(\text{AlAs})_6$ superlattice. The wave vectors \mathbf{k} are in units of $2\pi/(\text{lattice constant})$. For each superlattice state, the coefficients, normalized so that the largest coefficient is 1, are shown separately for the top three pairs of spin-degenerate bulk valence bands (VB2, VB3, and VB4) and for the bottom two pairs of spin-degenerate bulk conduction bands (CB1 and CB2). The labeling is such that VB2 corresponds to the bulk split-off bands, VB3 corresponds to the bulk light-hole bands, VB4 corresponds to the bulk heavy-hole bands, and CB1 corresponds to the lowest conduction bands. It should be noted that (i) the coefficients for the conduction states show strong mixing across the bulk Brillouin zone, (ii) state V1 has no contributions from the bulk conduction bands, and (iii) strong mixing occurs between most of the superlattice valence states. Note that the first-excited light-hole-like state V5 lies above the Γ_8^v (AlAs) barrier (see Fig. 2).

\mathbf{k}	VB2	VB3	VB4	CB1	CB2
(C3) ground zone-center-related state					
(0,0,0.000)	0.0000	0.0000	0.0000	1.0000	0.0000
(0,0,0.166)	0.0020	0.0001	0.0000	0.0667	0.0005
(0,0,0.333)	0.0001	0.0000	0.0000	0.0003	0.0010
(0,0,0.500)	0.0002	0.0000	0.0000	0.0058	0.0003
(0,0,0.666)	0.0000	0.0000	0.0000	0.0318	0.0004
(0,0,0.833)	0.0000	0.0000	0.0000	0.1056	0.0014
(0,0,1.000)	0.0000	0.0000	0.0000	0.0038	0.0005
(C2) first-excited zone-edge-related state					
(0,0,0.000)	0.0002	0.0002	0.0002	0.4581	0.0000
(0,0,0.166)	0.0009	0.0001	0.0000	0.0256	0.0011
(0,0,0.333)	0.0003	0.0000	0.0000	0.0017	0.0041
(0,0,0.500)	0.0001	0.0000	0.0000	0.0041	0.0008
(0,0,0.666)	0.0002	0.0000	0.0000	0.1917	0.0039
(0,0,0.833)	0.0001	0.0000	0.0000	0.9998	0.0040
(0,0,1.000)	0.0000	0.0000	0.0000	0.0301	0.0078
(C1) ground zone-edge-related state					
(0,0,0.000)	0.0000	0.0000	0.0000	0.0237	0.0004
(0,0,0.166)	0.0005	0.0000	0.0000	0.0075	0.0010
(0,0,0.333)	0.0001	0.0000	0.0000	0.0019	0.0012
(0,0,0.500)	0.0001	0.0000	0.0000	0.0075	0.0026
(0,0,0.666)	0.0000	0.0000	0.0000	0.0099	0.0018
(0,0,0.833)	0.0001	0.0000	0.0000	0.9040	0.0021
(0,0,1.000)	0.0000	0.0000	0.0000	1.0000	0.0013
(V1) ground heavy-hole-like state					
(0,0,0.000)	0.0004	0.7777	1.0000	0.0000	0.0000
(0,0,0.166)	0.0000	0.0013	0.3629	0.0000	0.0000
(0,0,0.333)	0.0000	0.0002	0.0063	0.0000	0.0000
(0,0,0.500)	0.0000	0.0000	0.0008	0.0000	0.0000
(0,0,0.666)	0.0000	0.0000	0.0001	0.0000	0.0000
(0,0,0.833)	0.0000	0.0000	0.0000	0.0000	0.0000
(0,0,1.000)	0.0000	0.0000	0.0000	0.0000	0.0000
(V2) ground light-hole-like state					
(0,0,0.000)	0.0136	0.0918	1.0000	0.0000	0.0000
(0,0,0.166)	0.0131	0.0924	0.0012	0.0004	0.0001
(0,0,0.333)	0.0000	0.0011	0.0001	0.0000	0.0000
(0,0,0.500)	0.0000	0.0002	0.0000	0.0001	0.0001
(0,0,0.666)	0.0000	0.0000	0.0000	0.0000	0.0000
(0,0,0.833)	0.0000	0.0000	0.0000	0.0001	0.0000
(0,0,1.000)	0.0000	0.0000	0.0000	0.0000	0.0000
[V3 (mixed with V4)] first-excited heavy-hole-like state					
(0,0,0.000)	0.4987	0.0080	0.0535	0.0000	0.0003
(0,0,0.166)	0.0218	0.0568	1.0000	0.0001	0.0001
(0,0,0.333)	0.0000	0.0008	0.1267	0.0000	0.0000
(0,0,0.500)	0.0000	0.0002	0.0018	0.0001	0.0001
(0,0,0.666)	0.0000	0.0000	0.0009	0.0000	0.0000
(0,0,0.833)	0.0000	0.0000	0.0000	0.0000	0.0000
(0,0,1.000)	0.0000	0.0000	0.0001	0.0000	0.0000

TABLE II. (Continued).

\mathbf{k}	VB2	VB3	VB4	CB1	CB2
		[V4 (mixed with V3)]			
		ground split-off state			
(0,0,0.000)	1.0000	0.0086	0.0613	0.0000	0.0000
(0,0,0.166)	0.0354	0.1394	0.2014	0.0002	0.0002
(0,0,0.333)	0.0000	0.0061	0.0243	0.0000	0.0000
(0,0,0.500)	0.0001	0.0000	0.0003	0.0001	0.0001
(0,0,0.666)	0.0000	0.0001	0.0002	0.0000	0.0000
(0,0,0.833)	0.0000	0.0000	0.0000	0.0001	0.0000
(0,0,1.000)	0.0000	0.0000	0.0000	0.0000	0.0000
		[V5 (mixed with V6)]			
		first-excited light-hole-like state			
(0,0,0.000)	0.0000	0.0232	0.0277	0.0014	0.0000
(0,0,0.166)	0.0004	1.0000	0.0827	0.0005	0.0000
(0,0,0.333)	0.0001	0.1150	0.0148	0.0000	0.0000
(0,0,0.500)	0.0000	0.0015	0.0011	0.0000	0.0000
(0,0,0.666)	0.0000	0.0008	0.0001	0.0000	0.0000
(0,0,0.833)	0.0000	0.0000	0.0001	0.0000	0.0000
(0,0,1.000)	0.0000	0.0001	0.0000	0.0000	0.0000
		[V6 (mixed with V5)]			
		ground heavy-hole-like resonant state			
(0,0,0.000)	0.0006	0.4378	0.4859	0.0002	0.0000
(0,0,0.166)	0.0003	0.1474	0.9992	0.0001	0.0000
(0,0,0.333)	0.0000	0.0272	0.1290	0.0000	0.0000
(0,0,0.500)	0.0000	0.0009	0.0105	0.0000	0.0000
(0,0,0.666)	0.0000	0.0001	0.0001	0.0000	0.0000
(0,0,0.833)	0.0000	0.0000	0.0004	0.0000	0.0000
(0,0,1.000)	0.0000	0.0000	0.0000	0.0000	0.0000

3 that the conduction states do not show envelope structures which are as distinct as those corresponding to the valence states. The best confined and least mixed states are V1 and V2 (the ground heavy-hole-like and ground light-hole-like states). It can be seen from Table II, that these states have little admixture from bulk bands other than the heavy- and light-hole bands. In contrast with this, states V5 and V6 show giant heavy-light-hole mixing at the anticrossings near $N=3$ and $N=7$. We also find that the heavy-hole-like state V4 and the light-hole-like state V6 near $N=10$ (see Fig. 2) contain large bulk split-off components. Table II also shows that the conduction states couple more strongly to the split off than the heavy- and light-hole bands. This feature has also been demonstrated in the case of the GaSb-InAs (001) superlattice.⁸ It was shown that the effect of such coupling, easily interpreted within the framework of a perturbation expansion for the effective mass m^* of the ground zone-center-related conduction state, is to reduce m^* and so allow increased penetration into the barrier region. In the case of the GaAs-AlAs system, any reduction in the effective mass of the ground zone-center-related conduction state due to coupling to the split-off bands is insignificant compared with the increases in effective mass due to zone-center-zone-edge mixing.

In Fig. 4, we show the charge densities of the valence states closest to the band edge for the case $M=1$, $N=11$. For this superlattice, the width of the GaAs layer is about 2.5 Å and the width of the AlAs layer is about 31.5 Å. The coefficients in the expansion of the wave functions

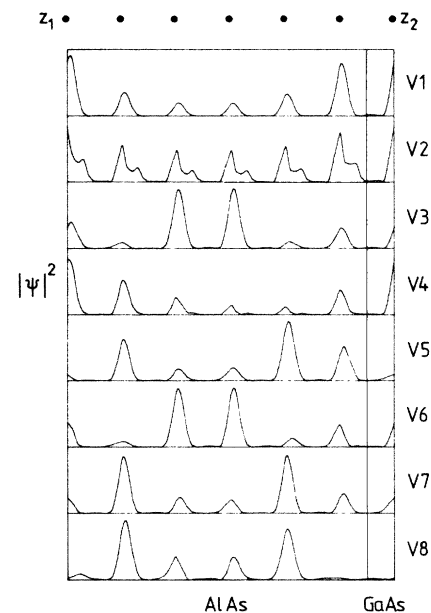


FIG. 4. Charge densities of the states at the top of the valence band at the center of the superlattice Brillouin zone for the $(\text{GaAs})_1(\text{AlAs})_{11}$ superlattice. The charge densities are plotted along the line Z_1Z_2 in the [001] direction [see Fig. 1(a)]. The mid-bond positions through which the line passes are indicated at the top of the figure. The energies of the states are shown in Fig. 2 at $N=11$.

corresponding to the charge densities shown in Fig. 4 are very similar to those shown in Table II. It can be seen from Fig. 4, that the envelopes of states V1 and V2 still behave like the corresponding states in the simple Kronig-Penny model. Although the competing effects of the widths of the constituent layers dominate the structure and energies of the superlattice states, the spectral characters (i.e., the distribution of $A_{n\mathbf{k}_s}$ weightings in bulk wave-vector space) are determined essentially by the property of periodicity which is embodied in the superlattice system. In the case of states V1, V2, and V4, the periodicity also controls the integrity of the charge density. It can be seen from Fig. 2, that states V3 and V5 at $N=11$ lie below the $\Gamma_8^-(\text{AlAs})$ level. These states are identified as the ground and first-excited heavy-hole-like resonant states since their charge is located mostly in the AlAs layers. Similarly, states V6 and V7 are identified as the ground and first-excited light-hole-like resonant states.

In order to give further insight into the form of the superlattice states in Fig. 4, we have plotted the (pseudo) charge densities along the spiral of bonds between the (pseudo) atoms in the unit cell. The charge densities are shown in Fig. 5. Bearing in mind that the states at the top of the valence band are bonding states and so most of their charge sits in between the atoms, it can be seen from Figs. 1 and 5 that the charge density of state V2 is preferentially localized in those bonds lying in the $\{101\}$ planes. The positions of the bonds are given by the peaks in the charge density of state V1. Polarized charge densities similar to those of state V2 have been observed by

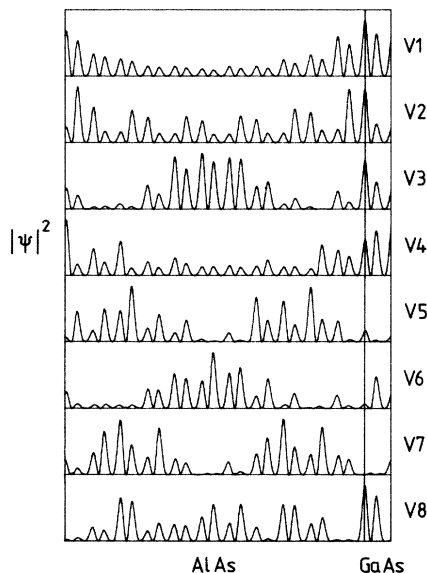


FIG. 5. Charge densities of the states at the top of the valence band at the center of the superlattice Brillouin zone for the $(\text{GaAs})_1(\text{AlAs})_{11}$ superlattice. The charge densities have been plotted along the spiral of bonds shown in Fig. 1. The states at the top of the valence band are p -like bonding states and their charge is located mostly on the bonds. The positions of the bonds are given by the peaks in the charge density of state V1. It can be seen that the charge in state V2 is localized mostly in those bonds lying in the $\{101\}$ planes.

Pickett *et al.*³ for the case of a GaAs-AlAs (110) superlattice comprised of ultrathin layers. The morphogenesis of charge density of the ground light-hole-like state (compare Fig. 3 with Fig. 4) occurs at $M=2$. The components of the charge density of state V2 in Fig. 4 have been analyzed in terms of their \mathbf{k}, n origin. It was found that the feature of charge channelling is not a result of mixing between superlattice states but appears to depend only on the widths of the constituent layers.

In addition to the case with $M=N=6$, we have also calculated the electronic structure of other $M=N$ superlattices and in Fig. 6 we show how our calculated superlattice energy gap (SEG) varies with N . We also show the SEG's at 4.2 K of Ishibashi *et al.* together with other relevant experimental data.^{1,21,22} It should be noted that the energy difference which we have calculated to give a value for the SEG is the difference in energy between one-electron states. Since exciton effects have not been included in the present calculations, our SEG would therefore be larger than the corresponding experimental SEG by an amount, probably less than about 20 meV,²³ corresponding to the unknown exciton binding energy. It can be seen from Fig. 6 that there is a plateau near $N=8$. We identify this as the crossing region of the zone-center- and zone-edge-related superlattice states. For $N \lesssim 8$, the lowest conduction state is a state which is derived primarily from the zone edge of AlAs. Excitonic effects in the superlattices with $N \lesssim 8$ are likely to be interesting

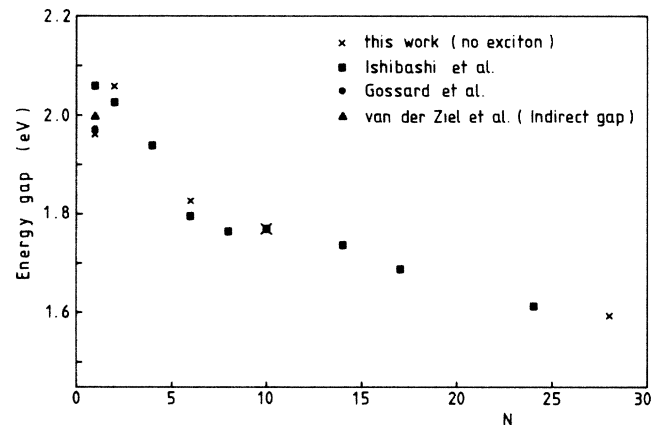


FIG. 6. Variation in the superlattice energy gap (SEG) with the number N of monolayers in the $(\text{GaAs})_N(\text{AlAs})_N$ (001) superlattices. The results obtained by Ishibashi *et al.* in addition to other relevant experimental data are shown together with the results of our calculations (Refs. 1,21, and 22). The plateau near $N=8$ corresponds to the crossing region of the ground zone-center-related and ground and first-excited zone-edge-related conduction states. The SEG for $N \lesssim 8$ corresponds to the difference in energy between the top heavy-hole-like state and the lowest conduction state, which is derived primarily from the lowest zone-edge-minima in the bulk conduction bands. The pseudodirect transition at $N=1$ has an oscillator strength which is comparable with the oscillator strength for the corresponding transition to the lowest zone-center-related state. This reflects the strong zone-folding effects occurring in these short-period superlattices (see Tables III and IV).

since the zone-center-related states at the top of the valence band and the zone-edge-related states at the bottom of the conduction band are confined predominantly in different layers. Due to very strong coupling between the zone-center and zone-edge bulk states, the oscillator strength for the transition from the top heavy-hole-like state to the ground zone-edge-related conduction state is comparable with or only about 1–3 orders of magnitude less than that for the same transition to the lowest zone-center-related conduction state. To illustrate this, we show in Table III the oscillator strengths for some of the transitions between relevant states (see also Fig. 7 and Table IV) in the $M=N=1$ superlattice. The effect of mixing Γ components into zone-edge-related states resulting in otherwise forbidden transitions becoming allowed is usually referred to as zone folding. In this case, it can be seen to arise because, in the sense of the Kronig-Penny model, the X well is sitting deep inside the Γ well. We suggest, therefore, that the transitions which Ishibashi *et al.*¹ have used to give the magnitude of the SEG for $N \lesssim 8$ is the pseudodirect transition ($V1 \rightarrow C1$). It is unclear why the photoluminescence from the $(\text{GaAs})_1(\text{AlAs})_1$ superlattice shows dramatic quenching compared with the other superlattices.¹ Perhaps quenching by defects such as trapping states may have been important in this structure. However, it should be noted that we have not allowed for possible reconstruction within our unit cell, a feature which may be important when the period of the superlattice is only one lattice constant.

In Fig. 8, we show the dispersion in the k_z direction of the lowest conduction states in the $(\text{GaAs})_1(\text{AlAs})_1$ and the $(\text{GaAs})_2(\text{AlAs})_2$ superlattices. The lowest three levels have been labeled symbolically according to the bulk zone minimum (at point Γ or X) from which they are primarily derived, although it is clear from Table IV that these states should not be considered as pure zone-edge or

TABLE III. Oscillator strengths for various transitions from states at the top of the valence band to states at the bottom of the conduction band in the $(\text{GaAs})_1(\text{AlAs})_1$ superlattice. State V1 is the ground heavy-hole-like state and state V2 is the ground light-hole-like state. States C1 and C2 are zone-edge-related states and state C3 is the ground zone-center-related state. These oscillator strengths illustrate the strong zone folding (transition V1/V2 to C1/C2 is allowed) and strong mixing between ground valence states (observable transitions from V1 with [001] polarization) which take place in this superlattice. See also Fig. 7 and Table IV.

Initial state	Final state		
	C1	C2	C3
		[110] polarization	
V1	2.304	0.284	2.019
V2	0.534	0.113	0.349
		[001] polarization	
V1	0.007	0.032	0.076
V2	2.372	0.217	2.576

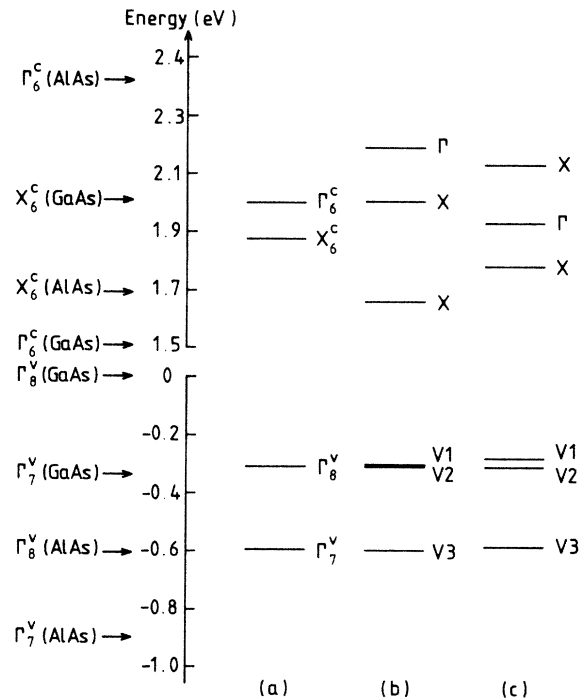


FIG. 7. Energy levels calculated for (a) the virtual crystal alloy $\text{Al}_{0.5}\text{Ga}_{0.5}\text{As}$, (b) the $(\text{GaAs})_1(\text{AlAs})_1$ superlattice, and (c) the $(\text{GaAs})_2(\text{AlAs})_2$ superlattice. The lowest three conduction levels in (b) and (c) have been labeled symbolically according to the principal bulk minima (Γ or X) from which they are primarily derived. The principal symmetry points of GaAs and AlAs are shown on the left of the figure. The label V1 denotes the ground heavy-hole-like state, the label V2 denotes the ground light-hole-like state and the label V3 denotes the ground split-off state.

zone-center states. It can be seen from Fig. 8(b), that the lowest conduction state has its minimum away from the zone center; this is a reflection of the fact that the secondary minima do not lie exactly at the edge of the BBZ. Even with 85:15 offsets, we find, in agreement with Andreoni and Car,⁵ that the lowest conduction state in the $(\text{GaAs})_2(\text{AlAs})_2$ superlattice is derived primarily from the edges of the BBZ. We note that in going from $M, N=2$ to $M, N=1$, the lowest conduction state drops down out of the X well and its dispersion along the k_z direction resorts to a near parabolic form near the zone center (see Fig. 8). We suggest that the superlattice at $M, N=1$ is behaving as though it were a new material whose energy levels cannot easily be interpreted within a framework which rests on the concept of band offsets. Indeed, it can be seen from Table IV, that the leading coefficients in the expansions of the lowest conduction states are not derived solely from one band. However, even for $M, N=1$ we find, in agreement with the experimental measurements of Gosard *et al.*,² that the optical matrix elements for transitions between the top valence states and the bottom conduction states at the center of the SBZ show anisotropy for polarizations normal to and parallel with the [001] direction (see Table III). Again, this is a property which

tire range of superlattices shown in Fig. 6 have been performed using potentials in which the 60:40 offset has been achieved by adjusting $V_L(q)$ at and near $q=0$. In reality, the actual offset is influenced by transfer of charge between the two materials which takes place in a narrow region at the interfaces. Such an effect, notoriously difficult to establish quantitatively,²⁴ has its origins in both

small and large q components of the potential. Since this problem has been temporarily circumvented by adjusting only the small q components of the potential, the results for superlattices comprising a few monolayers, in particular those for the $M, N=1$ superlattice, must be treated with caution. Also, it might be argued that the crystal potential in our calculations is not arrived at in an

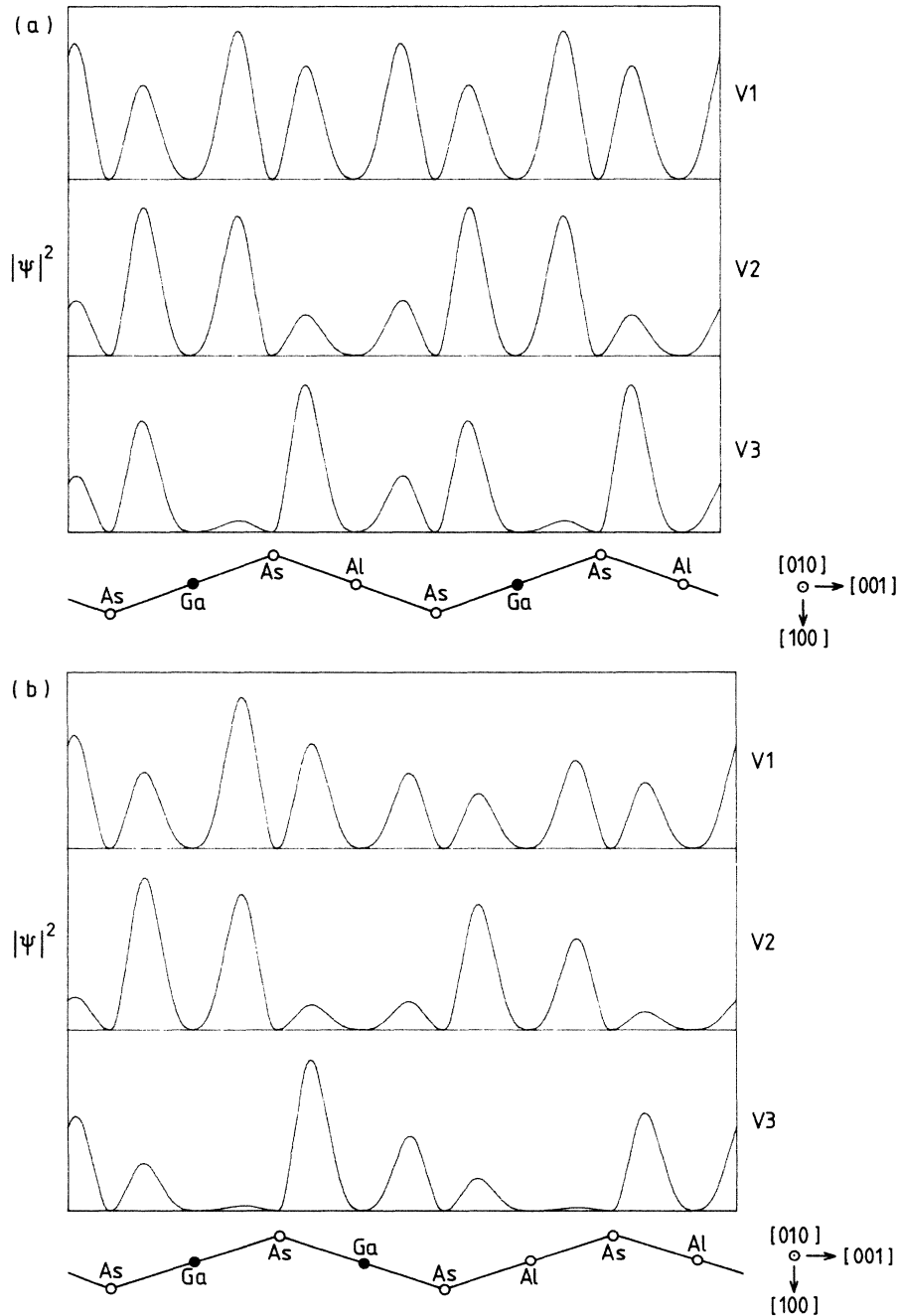


FIG. 9. Charge densities of the states at the top of the valence band in (a) the $(\text{GaAs})_1(\text{AlAs})_1$ superlattice and (b) the $(\text{GaAs})_2(\text{AlAs})_2$ superlattice. State V1 is the ground heavy-hole-like state, state V2 is the ground light-hole-like state, and state V3 is the ground split-off state. The charge densities have been plotted along a spiral of bonds joining (pseudo) atoms. In (a) the spiral has been extended across two unit cell in order to highlight the strong similarity between the two sets of charge densities. Note that in both superlattices, the ground light-hole-like state shows preferential localization in those bonds lying in the $\{101\}$ planes. The ground heavy-hole-like state in the $(\text{GaAs})_2(\text{AlAs})_2$ superlattice is beginning to show preferential localization in the GaAs region.

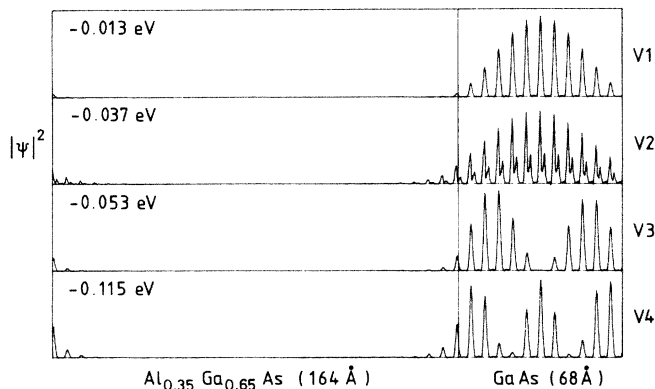


FIG. 10. Charge densities of the ground heavy-hole-like (V1), the ground light-hole-like (V2) and the first (V3) and second (V4) excited heavy-hole-like states at the center of the SBZ in the $(\text{GaS})_{24}(\text{Al}_{0.35}\text{Ga}_{0.65}\text{As})_{58}$ (001) superlattice. The charge densities have been plotted along a line in the [001] direction which passes through mid-bond positions. The energy of each state measured from $\Gamma_8^v(\text{GaAs})$ is shown at the top left-hand corner of each charge-density plot. The charge-density plot of state V2 is indicative of channeling along those bonds lying in the $\{101\}$ planes [compare with Figs. 1(b), 1(c), 4, and 5].

a priori way and so may not be physically correct. However, although we are describing covalent bonds with a method based on pseudoatom form factors, we do not find serious contradiction with experiment. The form factors have been adjusted to reproduce, in as good agreement with experiment as possible, the energy levels of the states lying nearest to the Fermi energies in the GaAs and AlAs crystals. It is these bulk states which dominate the wave functions of the states lying closest to the band edges of the superlattice which in turn are the states giving rise to the observed optical transitions. In any case, a rigorous implementation of, say, the density functional formalism for the energy range in question lies outside the applicability of present-day theory.

We have carried out a series of tests^{8,25} which show that any uncertainty in our potential at wave vectors lying far from the bulk reciprocal-lattice vectors is irrelevant provided that extreme care is taken to ensure that all input parameters accurately represent the symmetry of the system. It is, in addition to the component of the superlattice potential at the bulk reciprocal-lattice vector with $q=0$, the Fourier components at and clustered around the nonzero bulk reciprocal-lattice vectors which play the leading role in determining the charge densities. It is for these reasons that self-consistency does not appear to be a stringent requirement for the calculation of the electronic and optical properties of superlattice structures whose layers are a few of more lattice constants in width. Charge redistribution between the layers is restricted to a narrow region at the interfaces and the resultant sheet of redistributed charge controls an effectively sharp step in potential. Our pseudopotential method can therefore be used to fit transition energies from experimental data to within a few meV despite the uncertainties in the long-

wavelength Fourier components of the superlattice potential.²⁶

Bearing in mind the sparsity and scatter of the experimental data which are available, it would not be appropriate at this stage to quantify the band offsets for the GaAs-AlAs system. However, it is clear from our theoretical work and from the experimental data of Ishibashi *et al.*, that X_6^c of AlAs lies about 0.3 eV below X_6^c of GaAs for those superlattices in which each of the layers is comprised of several ($M, N \geq 4$) monolayers. This clearly rules out certain offsets which have been proposed in the literature.²⁷ For the superlattices with $M, N \lesssim 4$, the concept of viewing each layer as a bulk-like material is tenuous and in the limit $M, N = 1$ such a concept must be inappropriate since nearest monolayers are dissimilar. Finally, it is worth noting that both the polarization of the charge density of the ground light-hole-like states and the band offsets measured by Wang *et al.*²⁸ appear to be independent of the crystallographic orientation of the interfaces. The interface dipoles arising from the differences in electrostatic potential between the two materials which make up the superlattice must play the dominant role in controlling the band offsets. However, since these interface dipoles are probably intimately linked with bulk properties and since the polarized charge densities of the ground light-hole-like (and other) states are certainly linked with bulk properties,⁸ we suggest that there may be a common link.

IV. SUMMARY

In summary, we have used our pseudopotential method to show the strong mixing and zone-folding effects which occur in superlattices comprised of ultrathin layers when zone-center- and zone-edge-related states cross. We have presented a detailed comparison with the experimental data of Ishibashi *et al.*¹ and have indicated how the energetics of this crossing can be linked to the relative alignment between the GaAs and AlAs band structures. Specifically, we suggest that X_6^c of AlAs lies about 0.3 eV below X_6^c of GaAs. We suggest that the transitions which Ishibashi *et al.* have used to give the magnitude of the superlattice energy gap for the systems comprised of ultrathin layers is the pseudodirect transition. The fact that the oscillator strengths for transitions from the top heavy-hole-like state to the bottom zone-edge-related conduction state can be so large arises from strong zone folding. We have also shown that the superlattice periodicity governs the spectral character of the superlattice states and impresses optical anisotropy on the superlattice, even for those superlattices whose period is only two monolayers. The tetragonal symmetry of the superlattice determines a unique and highly restricted set of states in wave-vector space which can participate in the formation of the superlattice states and so confinement can occur in layers with only a few atoms even though the superlattice potential is not deep.

We illustrated a morphogenesis of charge density which is controlled by the way in which the superlattice period is divided up into the constituent layers. We showed that the polarized charge densities which may exist in superlat-

tices comprised of very thin and ultrathin layers may also be found in thick-layered systems. These states may have interesting transport properties.

It would seem that the concept of a band offset appears to hold even for superlattices whose period is only 3 or 4 lattice constants. The states at the edge of the valence band in systems with such narrow layers can be described in terms of momentum states close to the zone center and derived from a relatively narrow range of energies. Tables of relevant momentum components were presented which show a negligible mixing between valence and conduction bulk states. In contrast with earlier calculations,⁵ we find that the alternating monolayer superlattice is not concep-

tually equivalent to an alloy of the corresponding composition. Finally, a range of dispersion relations were presented as a function of the ratio of the GaAs layer width to the AlAs layer width which promise interesting opportunities for band-structure engineering.

ACKNOWLEDGMENTS

We wish to acknowledge financial support from the Science and Engineering Research Council, United Kingdom (M.A.G. and D.N.) and from the Royal Signals and Radar Establishment at Malvern (M.A.G.).

-
- ¹A. Ishibashi, Y. Mori, M. Itabashi, and M. Watanabe, *J. Appl. Phys.* **58**, 2691 (1985).
- ²E. Caruthers and P. J. Lin-Chung, *J. Vac. Sci. Technol.* **15**, 1463 (1978).
- ³W. E. Pickett, S. G. Louie, and M. L. Cohen, *Phys. Rev. B* **17**, 815 (1978).
- ⁴J. N. Schulman and T. C. McGill, *Phys. Rev. B* **19**, 6341 (1979).
- ⁵W. Andreoni and R. Car, *Phys. Rev. B* **21**, 3334 (1980).
- ⁶K. K. Mon, *Solid State Commun.* **41**, 699 (1982).
- ⁷M. Jaros, K. B. Wong, and M. A. Gell, *Phys. Rev. B* **31**, 1205 (1985).
- ⁸M. A. Gell, K. B. Wong, D. Ninno, and M. Jaros, *J. Phys. C* (to be published).
- ⁹G. Weisz, *Phys. Rev.* **149**, 504 (1966).
- ¹⁰S. Bloom and T. K. Bergstresser, *Solid State Commun.* **6**, 465 (1968).
- ¹¹D. J. Wolford and J. A. Bradley, *Solid State Commun.* **53**, 1069 (1985).
- ¹²See references in M. Neuberger, *Handbook of Electronic Materials*, (Plenum, New York, 1971), Vol. 2.
- ¹³W. M. Yim, *J. Appl. Phys.* **42**, 2854 (1971).
- ¹⁴A. Onton, in *Proceedings of the 10th International Conference on the Physics of Semiconductors, Cambridge, Mass., 1970*, edited by S. P. Keller, J. C. Hensel, and F. Stern (U.S. AEC Div. Tech. Information, Oak Ridge, Tenn., 1970), p. 107.
- ¹⁵R. C. Miller, D. A. Kleinman, and A. C. Gossard, *Phys. Rev. B* **29**, 7085 (1984).
- ¹⁶W. I. Wang, E. E. Mendez, and F. Stern, *Appl. Phys. Lett.* **45**, 639 (1984).
- ¹⁷H. Okumura, S. Misawa, S. Yoshida, and S. Gonda, *Appl. Phys. Lett.* **46**, 377 (1985).
- ¹⁸R. C. Miller, A. C. Gossard, and D. A. Kleinman, *Phys. Rev. B* **32**, 5443 (1985).
- ¹⁹M. H. Meynadier, C. Delalande, G. Bastard, M. Voos, F. Alexandre, and J. L. Lievin, *Phys. Rev. B* **31**, 5539 (1985).
- ²⁰J. Batey, S. L. Wright, and D. J. DiMaria, *J. Appl. Phys.* **57**, 484 (1985).
- ²¹A. C. Gossard, P. M. Petroff, W. Wiegmann, R. Dingle, and A. Savage, *Appl. Phys. Lett.* **29**, 323 (1976).
- ²²J. P. van der Ziel and A. C. Gossard, *J. Appl. Phys.* **48**, 3018 (1977).
- ²³R. C. Miller and D. A. Kleinman, *J. Lumin.* **30**, 520 (1985).
- ²⁴W. R. Frensley and H. Kroemer, *Phys. Rev. B* **16**, 2642 (1977).
- ²⁵M. Jaros, K. B. Wong, M. A. Gell, and D. J. Wolford, *J. Vac. Sci. Technol. B* **3**, 1051 (1985).
- ²⁶D. Ninno, M. A. Gell, and M. Jaros, *J. Phys. C* (to be published).
- ²⁷R. Dingle, in *Festkörperprobleme, edited by H. J. Queisser* (Vieweg, Braunschweig, 1975), Vol. 15, p. 21.
- ²⁸W. I. Wang, T. S. Kuan, E. E. Mendez, and L. Esaki, *Phys. Rev. B* **31**, 6890 (1985).